A&A 376, 966–977 (2001)
DOI: 10.1051/0004-6361:20011010

Astronomy & Astrophysics

BVR photometry and Hα spectroscopy of RS CVn type binary MM Herculis⋆

G. Taş[1], S. Evren[1], G. Marino[2], A. Frasca[2], C. İbanoğlu[1], and S. Catalano[2]

[1] Ege University Observatory, Bornova, İzmir, Turkey
e-mail: tas, sevren, ibanoglu@astronomy.sci.ege.edu.tr
[2] Osservatorio Astrofisico di Catania, via S. Sofia 78, 95123 Catania, Italy
e-mail: gma@sunct.ct.astro.it; afr@sunct.ct.astro.it; scat@sunct.ct.astro.it

Received 3 April 2001 / Accepted 26 June 2001

Abstract. The RS CVn type eclipsing binary MM Herculis was observed photo-electrically using B, V and R filters in 1998 and 1999 and the light and colour curves were obtained. Spectroscopic observations were carried out in 1999. The new light and colour curves are anti-correlated with the observations of 1997, i.e. the system is bluer when it is faintest. The variations of the brightnesses at each special phase (0.0, 0.25, 0.5, and 0.75) show an almost cyclic change with a period of about 6 years. This value is in good agreement with the migration periods of the spots suggested by us previously. The outside-of-eclipse wave in the light curve shows a minimum at phase ≈0.50, and the mean colour of the system is the bluest at the same phase. When the spots located on the cooler component are seen around phase 0.50, the amplitude of the light variation outside eclipse is larger than the others. Such variation may be caused by the effect of the hotter component. Spectroscopic observations of the system were carried out in the spectral range 5860–6700 Å. The subtraction of a "synthetic" spectrum, built up with spectra of inactive standard stars, allows us to detect an Hα emission excess only from the cool component. New radial velocity measurements of the system were obtained and analyzed for the orbital parameters.

Key words. activity – MM Her – late type – starspots

1. Introduction

The RS CVn-type eclipsing binary MM Her (BD +22° 3245, G2 V+K0 IV, $V_{\max} = 9\overset{\mathrm{m}}{.}5, P_{\mathrm{orb}} = 7\overset{\mathrm{d}}{.}96$) was first observed visually by Tsesevich (1954) and, later, its light variations were discussed by many different authors (e.g. Sowell et al. 1983; Evren 1985, 1987a, 1987b; Heckert & Ordway 1995; Evren & Taş 1999; Taş et al. 1999). MM Her shows an outside-of-eclipse wave-like distortion which is one of the main characteristics for RS CVn-type binaries. The migration period of the wave-like distortion was calculated by different investigators to be between 3 and 8 years. Taş et al. (1999) (hereafter Paper I) have given two migration periods by considering the effect of two spots with a period of about 6 years. They also showed that the light (in V) and colour (in $B-V$) curves vary in anti-correlation. In general, the light and colour variations occur at the same phase in binaries of these type, and the active star is redder when it is at the minimum light, in agreement with the hypothesis of cool starspots as the cause of light variation. Conversely, in the case of MM Her, at the minimum light the colour of the system is bluer. Therefore, we proposed that the blueing in $B-V$ colour may arise from the photospheric bright facular structures that surround starspots. Evidence of $B-V$ and, more strongly, $U-B$ color curves correlated with the V light curve have been provided for other very active systems, like UX Ari and HR 1099 (see e.g. Catalano et al. 1996). U excess in active systems correlated with the activity level has been discussed by Amado & Byrne (1997) and ascribed to faculae prominent in the near-UV continuum. Recently, the new BVR light curves obtained from photoelectric observations made in 1998 and 1999 were published by Taş (2000a).

MM Her has also been studied spectroscopically by Imbert (1971), Popper (1988) and Hall & Ramsey (1992), and they found the γ velocity as $-50.8\ \mathrm{km\,s^{-1}}$, $-51.5\ \mathrm{km\,s^{-1}}$ and $-54.2\ \mathrm{km\,s^{-1}}$, respectively.

In this paper, we focus on the long-term photometric behaviour, cyclic variations in the brightnesses and new Hα spectroscopy of the system. Section 2 summarizes the observations and calculations. In Sect. 3, we present some results which were obtained from the light curves and some evidence for the activity of the cooler component. Section 4 is devoted to the spectroscopic results.

Send offprint requests to: S. Evren,
e-mail: sevren@astronomy.sci.ege.edu.tr

⋆ Based on observations collected at the Ege University Observatory, Turkey, and at the Catania Astrophysical Observatory, Italy.

The variations of the equivalent width and the Hα emission are discussed and a new radial velocity curve obtained and analyzed for the orbital parameters presented. The last section contains conclusions.

2. Observations

2.1. Photometry

The RS CVn type eclipsing binary MM Herculis was observed in B, V and R filters of the UBV system on 42 nights from May 5th to October 8th in 1998 and on 45 nights from March 1st to October 6th in 1999 at the Ege University Observatory. A total of 749 and 912 observational points were obtained in each colour in 1998 and 1999, respectively. The observations were made with the 48-cm Cassegrain telescope to which an SSP5A type photometer, including an unrefrigerated Hamamatsu R4457 PMT, was attached. The stars BD +21°3274 and BD +22°3250 were taken as comparison and check stars, respectively. The differential magnitudes, in the sense of variable minus comparison, were corrected for atmospheric extinction and the observed times were reduced to the Sun's center. No variability in the light of the comparison star was detected. Later on the brightness and colour of the comparison star were transformed to the standard system and these standard values have been given in Paper I. The standard deviation of each observed point is approximately $\pm 0\overset{\mathrm{m}}{.}005$. The new light elements of the system have been taken from Taş (2000b) as:

$$\mathrm{Min\ I} = \mathrm{JD(Hel)}\ 2\,445\,551.4274 + 7\overset{\mathrm{d}}{.}960326\ E. \qquad (1)$$

The cooler and more massive component of MM Her is at the inferior conjunction (closer to the observer) at phase zero. These elements have been used in all the calculations pertaining to the observations. The nightly mean magnitudes and colours obtained outside eclipses from 1998 to 1999 are given in Table 1. There are 33 and 28 observing nights outside eclipses in 1998 and 1999, respectively. In this table the columns present heliocentric time, phase, magnitude in V, colour in $B-V$ and $V-R$. The standard deviation of each measurement was also given in this table.

2.2. Spectroscopy

The spectroscopic observations were carried out between July 19 and 30, 1999 and between August 16 and September 5, 1999 at Catania Astrophysical Observatory (Mt. Etna, Italy) with the REOSC echelle spectrograph fed by the 91-cm telescope through an UV-NIR fiber of 200 μm core diameter. High-resolution spectroscopy was obtained by using the echelle cross-dispersion configuration based on a 900 lines/mm echellette grating and an echelle grating with 79 lines/mm.

The data were acquired with a 1100 × 1100 SITe thinned back-illuminated CCD of 24 × 24 μm pixel size, yielding a spectral range (in 5 orders) of approximately 5860 Å to 6700 Å, and a dispersion of 0.16 Å per pixel.

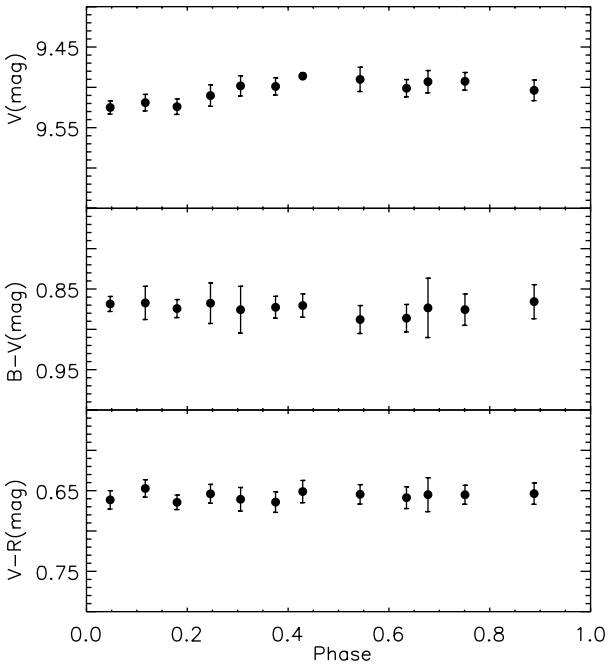

Fig. 1. The light and colour ($B-V$ and $V-R$) variations outside eclipses for 1998.

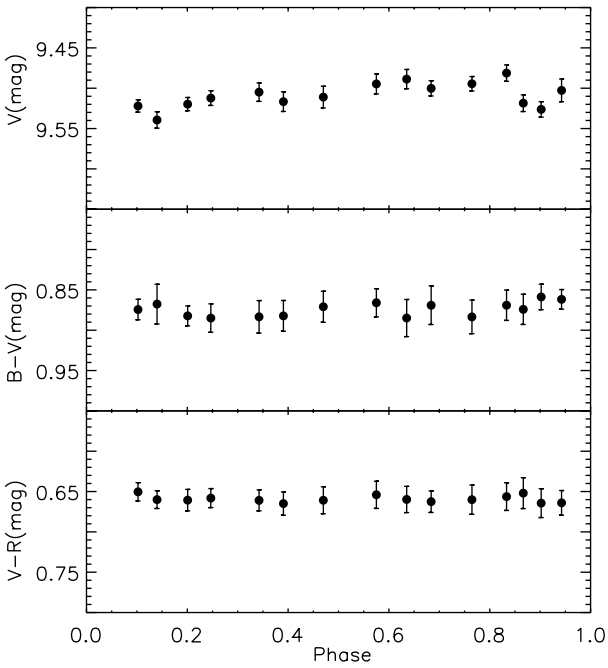

Fig. 2. The same as in Fig. 1, but for 1999.

For all observing runs the width of the slit was set to be 550 μm, projected onto 2.7 pixels of the detector, providing a spectral resolving power $\lambda/\Delta\lambda = 14\,000$. The signal-to-noise ratio *(S/N)* achieved is between 30 and 50, depending on atmospheric condition.

Sixteen spectra of MM Her were collected during 11 observing nights. We used 51 Peg (G2.5 IV) and δ Eri (K0 IV) as standard stars for hotter and cooler component, respectively. Typical exposure times for the MM Her

Table 1. The nightly mean magnitudes and colour of MM Her for 1998 and 1999.

1998					1999				
HJD	Phase	V	$B-V$	$V-R$	HJD	Phase	V	$B-V$	$V-R$
(2 400 000+)		(mag)	(mag)	(mag)	(2 400 000+)		(mag)	(mag)	(mag)
50939.4210	0.8559	9.497 ± 007	0.876 ± 010	0.658 ± 011	51239.5278	0.5562	9.498 ± 014	0.869 ± 024	0.663 ± 013
50949.4271	0.1129	9.509 ± 007	0.871 ± 033	0.633 ± 007	51250.5293	0.9382	9.503 ± 007	0.858 ± 015	0.650 ± 016
50941.4296	0.1082	9.523 ± 007	0.868 ± 014	0.651 ± 011	51240.5429	0.6837	9.500 ± 009	0.869 ± 024	0.663 ± 013
50949.4271	0.1129	9.509 ± 007	0.871 ± 033	0.633 ± 007	51250.5293	0.9382	9.503 ± 007	0.871 ± 018	0.654 ± 019
50955.5042	0.8763	9.510 ± 016	0.865 ± 016	0.664 ± 016	51313.3763	0.8333	9.481 ± 010	0.869 ± 019	0.660 ± 009
50951.4458	0.3665	9.503 ± 011	0.870 ± 013	0.668 ± 016	51290.3979	0.9467	9.503 ± 021	0.853 ± 007	0.668 ± 022
50954.4756	0.7471	9.499 ± 014	0.873 ± 026	0.657 ± 014	51295.4038	0.5755	9.491 ± 011	0.867 ± 015	0.654 ± 019
50955.5042	0.8763	9.510 ± 016	0.865 ± 016	0.664 ± 016	51313.3763	0.8333	9.481 ± 010	0.869 ± 019	0.656 ± 017
50957.4255	0.1177	9.521 ± 014	0.861 ± 016	0.656 ± 010	51325.3889	0.3423	9.505 ± 011	0.883 ± 020	0.661 ± 013
50958.4144	0.2419	9.510 ± 011	0.869 ± 018	0.653 ± 013	51327.3879	0.5935	9.495 ± 013	0.882 ± 012	0.661 ± 013
50967.3644	0.3662	9.504 ± 006	0.876 ± 011	0.669 ± 007	51339.3985	0.1023	9.522 ± 008	0.873 ± 023	0.658 ± 015
50962.4169	0.7447	9.487 ± 014	0.881 ± 020	0.659 ± 015	51332.2220	0.2007	9.520 ± 008	0.882 ± 012	0.661 ± 013
50967.3644	0.3662	9.504 ± 006	0.876 ± 011	0.669 ± 007	51339.3985	0.1023	9.522 ± 008	0.874 ± 013	0.650 ± 011
50970.4063	0.7484	9.493 ± 008	0.876 ± 016	0.651 ± 010	51342.3246	0.4698	9.511 ± 013	0.871 ± 019	0.661 ± 017
50974.3519	0.2441	9.514 ± 015	0.868 ± 039	0.657 ± 008	51348.4331	0.2372	9.516 ± 008	0.884 ± 012	0.663 ± 013
50977.4044	0.6275	9.501 ± 011	0.883 ± 015	0.657 ± 012	51369.3630	0.8665	9.519 ± 010	0.874 ± 019	0.652 ± 019
50979.4068	0.8790	9.499 ± 010	0.874 ± 016	0.653 ± 009	51372.4189	0.2504	9.514 ± 006	0.876 ± 023	0.661 ± 008
50982.3771	0.2522	9.507 ± 014	0.866 ± 019	0.651 ± 013	51376.3977	0.7502	9.484 ± 010	0.890 ± 028	0.666 ± 021
50989.3485	0.1279	9.523 ± 013	0.869 ± 020	0.648 ± 015	51379.4154	0.1293	9.535 ± 010	0.868 ± 022	0.661 ± 013
51001.3352	0.6337	9.511 ± 013	0.889 ± 019	0.670 ± 020	51381.4044	0.3792	9.518 ± 010	0.886 ± 017	0.662 ± 014
51010.3256	0.7632	9.492 ± 008	0.873 ± 016	0.653 ± 008	51388.3567	0.2526	9.507 ± 013	0.894 ± 017	0.650 ± 014
51015.3367	0.3927	9.490 ± 015	0.873 ± 017	0.656 ± 016	51407.3052	0.6329	9.490 ± 010	0.885 ± 016	0.663 ± 015
51017.3324	0.6434	9.491 ± 009	0.886 ± 017	0.649 ± 009	51411.3788	0.1447	9.541 ± 015	0.869 ± 028	0.659 ± 015
51019.3740	0.8998	9.506 ± 006	0.866 ± 032	0.649 ± 011	51415.3030	0.6374	9.487 ± 014	0.885 ± 030	0.657 ± 018
51027.3169	0.8976	9.499 ± 018	0.861 ± 023	0.641 ± 015	51421.2948	0.3905	9.511 ± 015	0.882 ± 020	0.661 ± 016
51040.3382	0.5334	9.496 ± 012	0.886 ± 017	0.656 ± 010	51427.2617	0.1397	9.547 ± 010	0.870 ± 025	0.667 ± 008
51052.2745	0.0329	9.524 ± 011	0.868 ± 015	0.665 ± 014	51443.2350	0.1463	9.535 ± 005	0.863 ± 023	0.653 ± 008
51073.3145	0.6760	9.493 ± 008	0.868 ± 021	0.652 ± 013	51445.2716	0.4024	9.522 ± 011	0.879 ± 020	0.672 ± 013
51075.2527	0.9195	9.510 ± 019	0.853 ± 029	0.658 ± 018	51446.3100	0.5330	9.510 ± 012	0.880 ± 016	0.660 ± 015
51080.2899	0.5523	9.484 ± 018	0.890 ± 018	0.653 ± 014	51449.2513	0.9020	9.526 ± 010	0.859 ± 016	0.664 ± 018
51081.2970	0.6788	9.493 ± 020	0.878 ± 053	0.658 ± 030	51456.2300	0.7790	9.505 ± 008	0.878 ± 014	0.654 ± 015
51084.2287	0.0471	9.526 ± 008	0.872 ± 008	0.664 ± 010					
51092.3013	0.0612	9.525 ± 006	0.866 ± 005	0.656 ± 010					
51093.2442	0.1796	9.524 ± 010	0.874 ± 011	0.664 ± 009					
51094.2475	0.3057	9.498 ± 012	0.876 ± 029	0.661 ± 015					
51095.2292	0.4290	9.486 ± 004	0.871 ± 014	0.651 ± 014					

spectroscopic observations were 3600 and 4200 s. α Ari was observed as a radial-velocity standard star.

The reduction of data including bias, scattered light and flat field corrections, extraction of spectral orders and wavelength calibration was performed on the raw images with Image Reduction and Analysis Facilities (IRAF) distributed by NOAO[1]. For the wavelength calibration the emission lines of a Th-Ar lamp were used.

[1] IRAF is distributed by the National Optical Astronomy Observatory, which is operated by the Association of the Universities for Research in Astronomy, inc. (AURA) under cooperative agreement with the National Science Foundation.

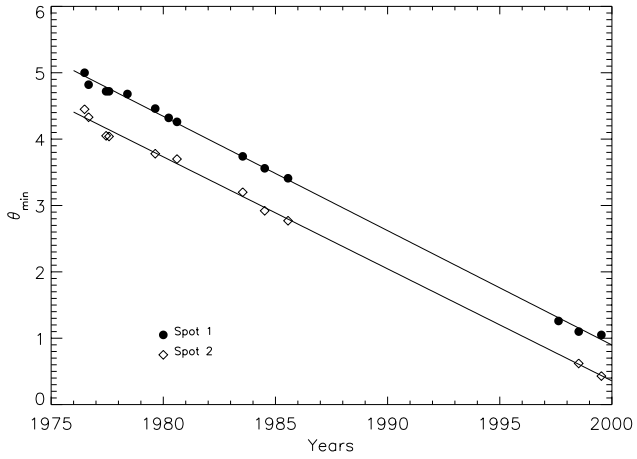

Fig. 3. The migration curves of the spots.

3. Photometric variation outside the eclipse

The mean light and colour variations obtained outside eclipse in 1998 and 1999 are shown in Figs. 1 and 2, respectively. From these figures it is clearly seen that the wave-like distortion generally has two minima and is asymmetrical in shape rather than being truly sinusoidal as it was in 1997 (Paper I). Therefore, it emerges that MM Her had at least two separate active regions in those years. In 1998 the first spot gives rise to the deeper minimum in the outside-of-eclipses light curve at phase 0.10, while the second spot is facing the observer at phase 0.62. Similar effects appeared around phases 0.05 and 0.43 in 1999, respectively. The amplitude of the light variation is about $0\overset{m}{.}04$ in 1998, it increased to about $0\overset{m}{.}05$ in 1999. The new light and colour curves also show anti-correlation as it appeared in the 1997 light and colour curves, i.e. the system is bluer at the phase of the wave minimum in the light curve. In Paper I, we tried to explain this behavior as the contribution to the total light and colour of the photospheric facular structures that surround starspots.

Long-term photometric observations allow us to search for active permanent longitudes on the RS CVn type stars. Long-lived active-longitude structures have been observed on several spotted stars like RS CVn, EI Eri, II Peg, σ Gem, HR 7275 and HK Lac (Rodonò et al. 1995; Berdyugina & Tuominen 1998; Berdyugina et al. 1999; Olah et al. 1991; Henry et al. 1995). The deepest minimum outside eclipses (in eclipsing binaries) or in the light curve (in non-eclipsing binaries) is caused by the largest active region (Spots Group 1 or Spot 1) on the cooler component. The shallower (secondary) minimum should correspond to smaller active region (Spots Group 2 or Spot 2). The displacement of the light minima in time gives us useful information about the migration of the active regions, spots or spot groups. The previous values given in Table 2 of Paper I and the new phases of the light minima ($\theta_{\min}$, as described in Paper I) for Spots 1 and 2 found in this study plotted against epoch are shown in Fig. 3. In the system's light curve obtained in 1997 (Paper I) the distortion effect of the second spot is not seen. The phase change of maximum visibility of the second spot in 1998 and 1999 provides an improvement of the migration period of Spot 2. Since no photometric observation of the system was obtained between 1985–1997, and the 1997 light and colour curve shows only the first spot, the new observations are very important to detect the migration period of the second spot. Applying a linear fit to the phase-shift, the following equations were re-obtained:

$$\theta_{\min} = -0.172 \times (t - 1900) + 18.13 \quad \text{forSpot 1} \qquad (2)$$
$$\pm 3 \qquad\qquad \pm 5$$

$$\theta_{\min} = -0.169 \times (t - 1900) + 17.23 \quad \text{forSpot 2} \qquad (3)$$
$$\pm 9 \qquad\qquad \pm 9$$

where t is in years. The mean time intervals required for Spot 1 and Spot 2 to sweep the light curve once were computed using Eqs. (2) and (3). If the $\theta_{\min}$s are replaced with integers corresponding to the start of the cycles, such as 3 and 4, the time differences between the corresponding years give the values for migration periods. Therefore, we found migration periods of 5.8 ± 0.1 years for Spot 1 and 5.9 ± 0.1 years for Spot 2. These values for the migration periods are in good agreement with that given in Paper I. The arrangement of the spots in two permanent strips can be easily interpreted as two long-lived active longitudes rotating practically at the same velocity.

The brightnesses outside the eclipses of the four different special phases (0.00, 0.25, 0.50 and 0.75) for data sets from Paper I and this study are presented in Table 2. To obtain the brightnesses at phases 0.00 and 0.50, the effects of the eclipses were first removed from the observed light curves, and then, the light and colour curves were represented with free-hand curves. V magnitudes at these special phases were read from the free-hand mean light curves which represent all the observed magnitudes quite well. The data presented in Table 2 are plotted in Fig. 4. The variations of the brightness at each special phase show an almost cyclic change with a period of about 6 years. This value is in good agreement with the migration periods of the spots previously estimated by us.

The amplitude of the brightness variations at each special phase ranges between $0\overset{m}{.}10$ and $0\overset{m}{.}15$ (see Fig. 4). The apparent visual magnitude of the system did not exceed $9\overset{m}{.}45$ at any special phase. However, it diminishes up to $9\overset{m}{.}60$ at phases 0.50 and 0.75. In the years in which the luminosities corresponding to each special phase are lowest, the wave-like distortion has a minimum at that phase. Therefore, the cyclic variations belonging to these phases are related to the spot migration.

The amplitudes of the light variations taken from Table 2 in Paper I and found in this study are plotted in Fig. 5 against the minimum phases of the wave-like distortions for each data set. When the variation is examined, a maximum is seen at phase ≈0.50. So if the spots seen at phase ≈0.50 are located on the cooler component of MM Her, they are on the hemisphere facing the companion. In principle there is no reason why these variations

Table 2. The V magnitudes of MM Her at four special phases for different data sets.

References	Mean Epoch	Phase 0.00	Phase 0.25	Phase 0.50	Phase 0.75
Sowell et al. (1983)	1976.49	0.900	0.900	0.900	0.895
Sowell et al. (1983)	1976.67	0.880	0.894	0.900	0.890
Sowell et al. (1983)	1977.45	0.860	0.889	0.850	0.852
Sowell et al. (1983)	1977.58	0.890	0.880	0.870	0.865
Sowell et al. (1983)	1978.40	0.880	0.885	0.880	0.870
Sowell et al. (1983)	1979.64	0.880	0.872	0.880	0.886
Sowell et al. (1983)	1980.24	0.900	0.878	0.870	0.885
Sowell et al. (1983)	1980.61	0.880	0.869	0.890	0.890
Evren (1986)	1983.54	0.840	0.870	0.840	0.860
Evren (1986)	1984.52	0.840	0.844	0.830	0.861
Evren (1986)	1985.56	0.860	0.838	0.830	0.851
Taş et al. (1999)	1997.63	0.880	0.859	0.870	0.891
This study	1998.52	0.863	0.871	0.881	0.876
This study	1999.53	0.862	0.884	0.878	0.875

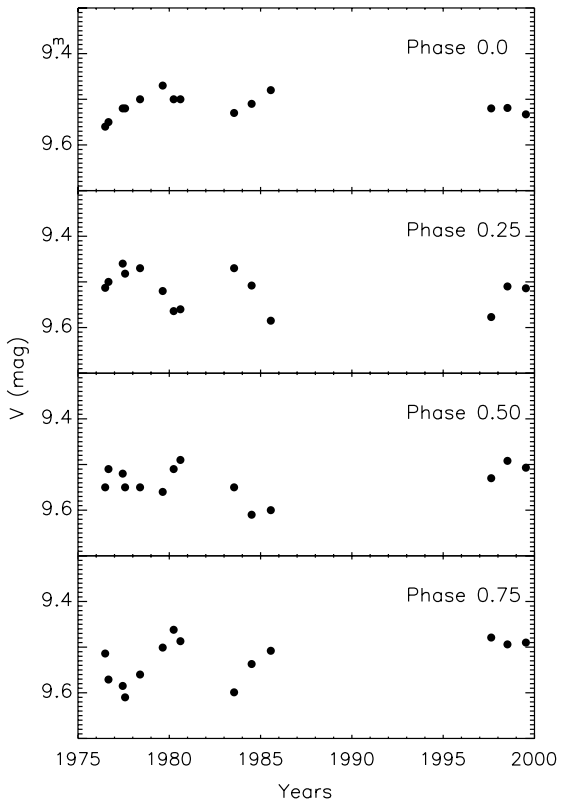

Fig. 4. The long-term variation of MM Her brightnesses at four special phases.

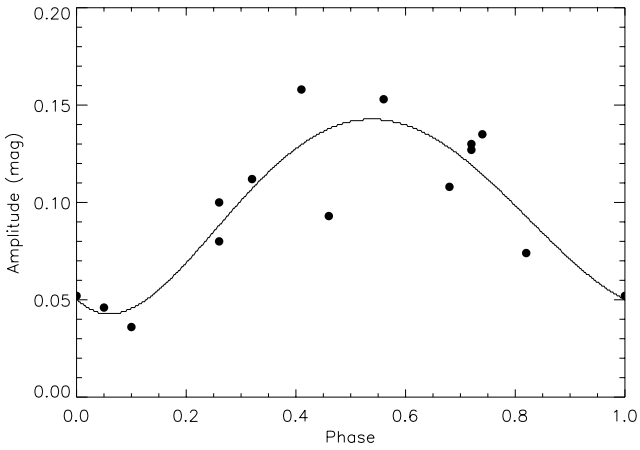

Fig. 5. The amplitudes of the light variations against the minimum phases of the wave-like distortions.

taking place in the vicinity of the secondary minimum should be more conspicuous than at other phases.

A similar behaviour was found in the light variation of II Peg by Berdyugina et al. (1999). They reported that the largest active region on the surface of II Peg shows the tendency to be closer to the secondary component of the binary and a long–standing concentration of spots on the hemisphere facing the companion has been found from light curve analysis of AR Lac (Lanza et al. 1998). Such variation may be caused by the effect of a secondary component in the system, i.e. the secondary seems to affect the magnetic activity of the primary and the spot parameters.

4. The radial velocity curve and the Hα line variation

4.1. Radial velocity curve of MM Herculis

The radial velocity measurements *(RV)* of MM Her were obtained by cross-correlation of each echelle order of MM Her spectra with spectra of the bright radial velocity standard star α Ari, whose radial velocity is $-14.3\,\mathrm{km\,s^{-1}}$ (Evans 1979). For this purpose we used FXCOR, which is one of the tasks of IRAF.

The wavelength ranges for the cross-correlation of MM Her spectra were selected in order to exclude the Hα

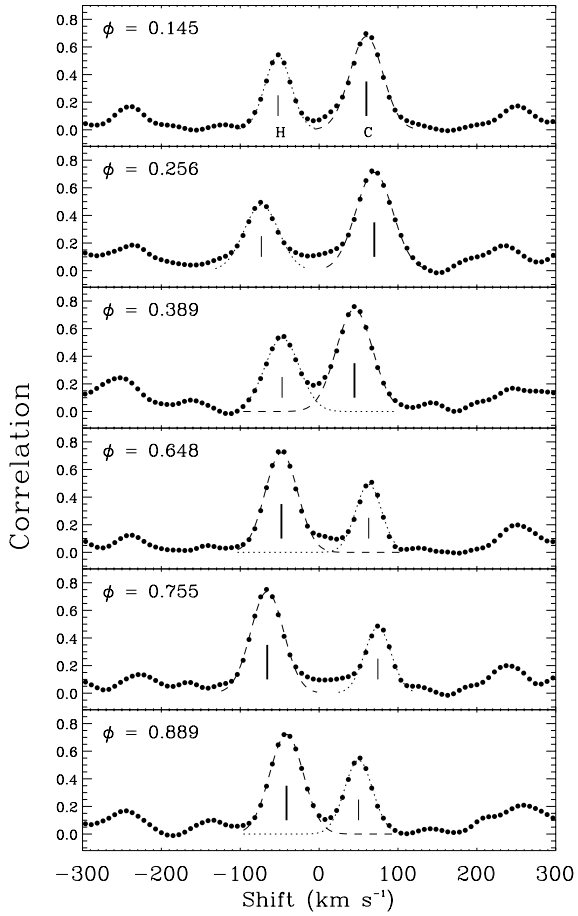

Fig. 6. Sample of Cross Correlation Functions (CCFs) between MM Her and template spectra (α Ari) at different phases (dots). The Gaussian fits to the two peaks are displayed with a dashed line for the K0 IV component and with a dotted line for the G2 IV one.

and Na I D_2 lines, which are contaminated by chromospheric emission. The spectral regions heavily affected by telluric lines (e.g. the λ 6276 − λ 6315 band of O_2) were also excluded.

Figure 6 shows examples of cross-correlation functions (CCFs) at various orbital phases. *RV*s of the two components have been obtained by a two-Gaussian fit to the CCFs.

The radial velocity measurements, listed in Table 3 together with their standard errors, are weighted means of the individual values deduced from each order. The usual weight $W_i = \frac{1}{\sigma_i^2}$ has been given to each measure.

The standard errors of the weighted means have been computed on the basis of the errors σ_i in the *RV* values for each order according the usual formula (see e.g. Topping 1972). The latter are computed by FXCOR according to the fitted peak height and the antisymmetric noise as described by Tonry & Davis (1979).

The observational points and the associated errors are displayed in Fig. 7 as a function of orbital phase (dots for the hotter star and open circles for the cooler one) as determined by means of the ephemeris based on the photometric times of primary eclipse (Eq. (1)). The sinusoidal solution (dashed and solid lines for the K0 and the G2 component respectively in Fig. 7), determined for a circular orbit, fits very well all the observations.

The orbital parameters of the system, derived from the radial velocity solution and from the solution of the light curve (Evren 1987b), are listed in Table 4, where c and h indices refer to the cooler and the hotter component of the system, respectively.

From blue-violet coudé spectrograms, Imbert (1971) found a systemic velocity of -50.8 ± 1.0 km s^{-1}. He deduced the velocities of the cooler component only from the Ca II H & K emission cores. Popper (1988) published radial velocity measurements essentially based on Lick blue-violet spectrograms. He measured the *RV* of the hotter star, which contributes about the 80% of the total light at these wavelengths, by means of several absorption lines, while he used the Ca II H & K emission lines for the cooler component, with the addition of few measurements performed onto red orticon spectra. From his own *RV*'s and a re-analysis of Imbert's data, he adopted $K_h = 74.0$ km s^{-1}, $K_c = 70.5$ km s^{-1} and $\gamma = -51.5 \pm 1.0$ km s^{-1}. Hall & Ramsey (1992), using 13 echelle spectra, found the systemic velocity to be -54.2 ± 3.3 km s^{-1}. Our systemic velocity ($\gamma = -52.6 \pm 0.2$ km s^{-1}) is consistent, within the errors, with previous determination reported above. So, it appears that the maximum variation of γ from 1967 (epoch of the first *RV* curve) up to now does not exceed 3.4 km s^{-1}.

The radial velocity amplitudes $K_h = 72.88$ km s^{-1}, and $K_c = 68.78$ km s^{-1} we obtain are a little smaller than the Imbert (1971) and Popper (1988) ones, but in good agreement with Hall & Ramsey (1992) values. Our mass ratio $q = 0.944$ leads to masses a little different from one another and as found by previous authors, but in better agreement with the spectral type (G2 V, K0 IV) and the evolutionary stage of the two components, i.e. the G2 component is still on the main sequence while the more massive K0 star has already become a subgiant.

4.2. Hα emission

The Hα line is an important indicator of chromospheric activity. It shows itself as an emission feature above the continuum in very active stars (e.g. II Peg, V711 Tau, UX Ari, XX Tri, AR Psc); in less active stars only a filled-in absorption line is observed.

The situation is more complex in a double-lined system in which both spectra are simultaneously seen and shifted at different wavelength, according to the orbital phase. Therefore, in order to extract a valid information about the chromospheric contribution a comparison is needed with a "synthetic" spectrum constructed with two stellar spectra that mimic the two components of the system in absence of activity.

For MM Her, the complete filling of the Hα line coming from the cooler component was first emphasized by

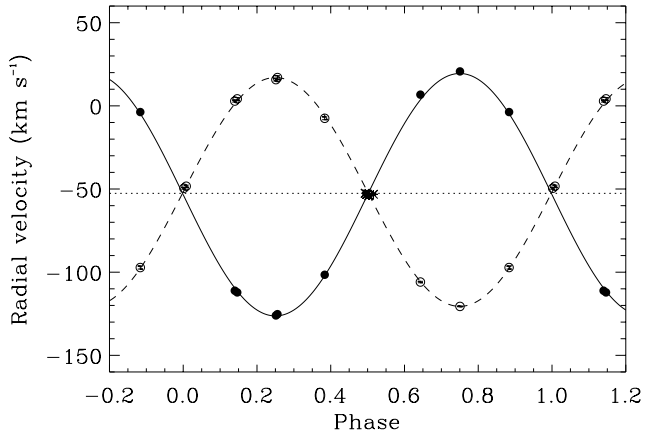

Fig. 7. The radial velocity curve of MM Her for 1999. Open circles: *RV*'s of the cool component. Filled circles: *RV*'s of the hotter one. Crosses: *RV* values obtained near the secondary eclipse, when the spectral lines of the two components are heavily blended. The error bars are always smaller than the symbol dimension and are barely visible inside the open circles. The best-fit solutions are drawn with dashed and continuous line for the cool and hot component, respectively.

Table 3. Radial velocity measurements of MM Her.

HJD (2 400 000+)	Phase	V_c (km s^{-1})	V_h (km s^{-1})
51380.4224	0.2558	15.76 ± 0.85	-126.03 ± 0.25
51381.4758	0.3881	-7.48 ± 0.86	-101.55 ± 1.26
51382.3496	0.4979	—	-52.53 ± 0.41
51382.3914	0.5032	—	-53.09 ± 0.26
51382.4332	0.5084	—	-54.00 ± 0.59
51384.3957	0.7550	-120.59 ± 0.25	20.72 ± 1.30
51385.4555	0.8881	-97.21 ± 0.89	-3.72 ± 1.55
51386.3972	0.0064	-49.54 ± 0.54	–
51386.4466	0.0126	-48.31 ± 0.64	–
51388.4165	0.2601	17.02 ± 1.11	-125.23 ± 1.54
51390.3442	0.5022	—	-53.17 ± 0.44
51390.3956	0.5087	—	-53.65 ± 0.45
51422.3309	0.5205	—	-53.17 ± 0.28
51423.3422	0.6475	-105.92 ± 0.43	6.75 ± 0.70
51427.2964	0.1443	2.88 ± 0.58	-111.13 ± 0.62
51427.3484	0.1508	4.21 ± 0.81	-112.17 ± 0.92

Table 4. New orbital parameters of MM Her.

γ (km s^{-1})	-52.59 ± 0.19
K_h (km s^{-1})	72.88 ± 0.23
K_c (km s^{-1})	68.78 ± 0.24
M_h/M_c	0.944 ± 0.005
$a_h \sin i$ (km)	$7.978\ 10^6 \pm 2.5 \times 10^4$
$a_c \sin i$ (km)	$7.529\ 10^6 \pm 2.7 \times 10^4$
$M_h \sin^3 i$ ($M_\odot$)	1.139 ± 0.009
$M_c \sin^3 i$ ($M_\odot$)	1.206 ± 0.009

Hall & Ramsey (1992) by means of the spectral synthesis technique. They also found in the difference spectra a faint emission feature corresponding to the G component at phases of good wavelength separation of the two lines, and a small extra-absorption at $\phi = 0.034$.

Montes et al. (1997) observed in MM Her a relevant emission excess from the Hα line of the cooler component, but no emission coming from the hotter one. They have no spectra near the primary eclipse.

We observed MM Her during eleven nights, acquiring a total of 16 spectra. In addition to MM Her, some inactive stars of spectral type similar to that of each component of the system have been observed. We have chosen 51 Peg (G2.5 IV) to reproduce the hotter component, and δ Eri (K0 IV) for the cooler one. The spectra of 51 Peg and δ Eri have been broadened by convolution with the appropriate rotational profile ($v \sin i = 10$ km s^{-1} and 18 km s^{-1} for the hot and cool component, respectively, Strassmeier et al. 1993a) and then have been coadded, properly weighted and Doppler-shifted according to the *RV* solution derived in the previous subsection.

The contributions of the two stars to the combined spectrum at the Hα wavelength have been evaluated from the relative areas of the Gaussians fitted to the cross-correlation peaks of each component (see Fig. 6). Average contributions of 0.40 and 0.60, for the hotter and cooler star respectively, have been obtained. These weights are in agreement with those derived from photometric elements (radii and effective temperatures) of the WINK solutions by Evren (1987b), in which a temperature of 5770 K has been assigned to the hotter component, in agreement with its spectral type and color indices.

During the eclipses these weights have been properly corrected, taking into account the light contribution of each star at each phase.

Furthermore, since the light of the cooler active star changes with phase due to starspots, the relative weights of the two components to the observed spectrum change accordingly. In order to also take into account this effect, we evaluated the true weights, deriving them from the simultaneous out-of-eclipse R light curve, corrected for the light offset of the inactive G star. The final weights of the cool component (w_C) for each observation phase are listed in Table 5. To define the net Hα emission of the two components we have subtracted the synthetic spectrum from each MM Her spectrum. In the difference spectrum the absorption lines cancel out and the excess emission of the cool component in the Hα core appears as a positive residual well above the noise (Fig. 8). In this figure, a sample of Hα profiles at different phases around the two quadratures is shown. In the left–hand panels the observed spectra are displayed by a thick line, while the thin line reproduces the synthetic ones. In the right–hand panels the differences are shown. The phases of observations and the wavelength of the Hα centers of the hot and cool component are also marked. Figure 9 displays a sample of spectra near to the two eclipses, together with the configuration

Table 5. Hα equivalent widths measurements of MM Her obtained in 1999.

HJD (2 400 000+)	Phase	w_C	EW (Å)
51380.4224	0.2558	0.574	0.664 ± 0.095
51381.4758	0.3881	0.582	0.665 ± 0.125
51382.3496	0.4979	0.410	0.415 ± 0.085
51382.3914	0.5032	0.421	0.486 ± 0.125
51382.4332	0.5084	0.446	0.495 ± 0.139
51384.3957	0.7550	0.600	0.749 ± 0.124
51385.4555	0.8881	0.587	0.741 ± 0.121
51386.3972	0.0064	0.953	1.328 ± 0.191
51386.4466	0.0126	0.813	0.995 ± 0.208
51388.4165	0.2601	0.574	0.634 ± 0.085
51390.3442	0.5022	0.413	0.383 ± 0.105
51390.3956	0.5087	0.448	0.477 ± 0.097
51422.3310	0.5205	0.550	0.548 ± 0.094
51423.3422	0.6475	0.599	0.751 ± 0.076
51427.2964	0.1443	0.571	0.616 ± 0.072
51427.3484	0.1508	0.571	0.653 ± 0.086

of the system at the observational phase, as viewed by an observer from Earth.

In the difference profile (Figs. 8, 9) we do not find any evidence of emission from the G2 V component, in agreement with Montes et al. (1997). The slight emission from the G2 V component claimed by Hall & Ramsey (1992) may result from the choice of the inactive standard star κ Del (G5 IV), whose spectrum does not well represent the G component of MM Her. Moreover, it seems that they do not take into account the change of the relative weights of the two stars due to the intrinsic variability of the K0 star; at least there is no mention made in their paper.

Our spectrum at phase 0.013, the closest to the one at $0^{\rm p}.034$, in which Hall & Ramsey (1992) found evidence of extra-absorption, does not show any sign of excess absorption. We do not find evidence of extra-absorption at any other phase.

The net equivalent width (EW) of the Hα emission has been evaluated on the difference spectra integrating along the residual emission profile. The errors on the measured EW were estimated determining the S/N in two windows on the right and left-hand side of Hα in the difference spectrum and multiplying it by the width of the integration range.

Equivalent widths (EW) calculated from emission excess are listed, together with their corresponding JD, phase, and weights, in Table 5.

Since these EWs are relative to the local continuum that is a mixture of the G and K star spectra whose weights vary with phase, to put the EW in a uniform scale in units of the K-star continuum, we need to correct these values dividing by its actual contribution to the composite spectrum (w_C). The corrected EWs are plotted versus orbital phase in Fig. 10. Different symbols have been used for in-eclipse values.

From Fig. 10 the EW measurements seem to vary with phase by about 0.15 Å, or about 14%, i.e. of the same size of the errors.

However, the average distribution of the corrected emission EW values (Fig. 10, upper panel) seems to indicate a lower emission at the first quadrature (phases $0.0 \div 0.5$) and a little higher emission at the second quadrature (phases $0.5 \div 1.0$). It is not clear if this difference is evidence of a real rotational modulation or the result of other effects.

In the lower panel of Fig. 10 we display the V light curve of MM Her obtained at the Ege University Observatory in 1999, at about the same time of the spectrographic observations. We can notice that the phase variation of the Hα emission is similar to that of the V light curve, i.e. the emission is higher at the phases at which the star is brighter. If this direct correlation is real, one has to suppose that the Hα faculae are more concentrated on the brighter hemisphere of the K star, and also that the V light maximum is due to faculae contribution. Although this anti–correlation will be clarified by UV observations, interpreting the Mg II or C IV line flux may indicate not only the presence of long–lived optical spot groups on one hemisphere of the cool component but also a corresponding long–lived plage region. This, however, is in contrast with the blueing in the $B-V$ at minimum light (Paper I) attributed to bright faculae overlaying the cool spots.

We have already analyzed the contemporaneous variation of Hα emission and the photometric wave in RS CVn binaries, finding in many cases that the higher emission occurs at the wave minimum, suggesting a close association of chromospheric plages with photospheric spots (Catalano et al. 1996, 2000). A similar solar-like scenario has been shown by several authors for active binaries (e.g. Weiler 1978; Bopp & Talcott 1978; Ramsey & Nations 1984; Rodonò et al. 1987; Doyle et al. 1989; Strassmeier 1994) as well as for single stars (Strassmeier et al. 1993b; Frasca et al. 2000b). But also cases of stars with a well defined photometric wave, that generally show normal solar-type correlation and sometimes do not show any Hα modulation, have been found (see Catalano et al. 2000).

Although a positive correlation between photometric wave and Hα emission in the present data of MM Her may not be excluded, we would like to remark that a similar difference of Hα emission at the two quadratures has been found for the G2 IV component of AR Lac (Frasca et al. 2000a). In the AR Lac case the effect was associated with the extra-absorption effect clearly detected in the Hα profile before and during primary eclipse. In the case of MM Her, evidence of extra-absorption have been found by Hall & Ramsey (1992) after the primary eclipse. The lower emission of the K0 IV component at the first quadrature seems to be consistent with extension of absorbing matter above the trailing hemisphere of that star.

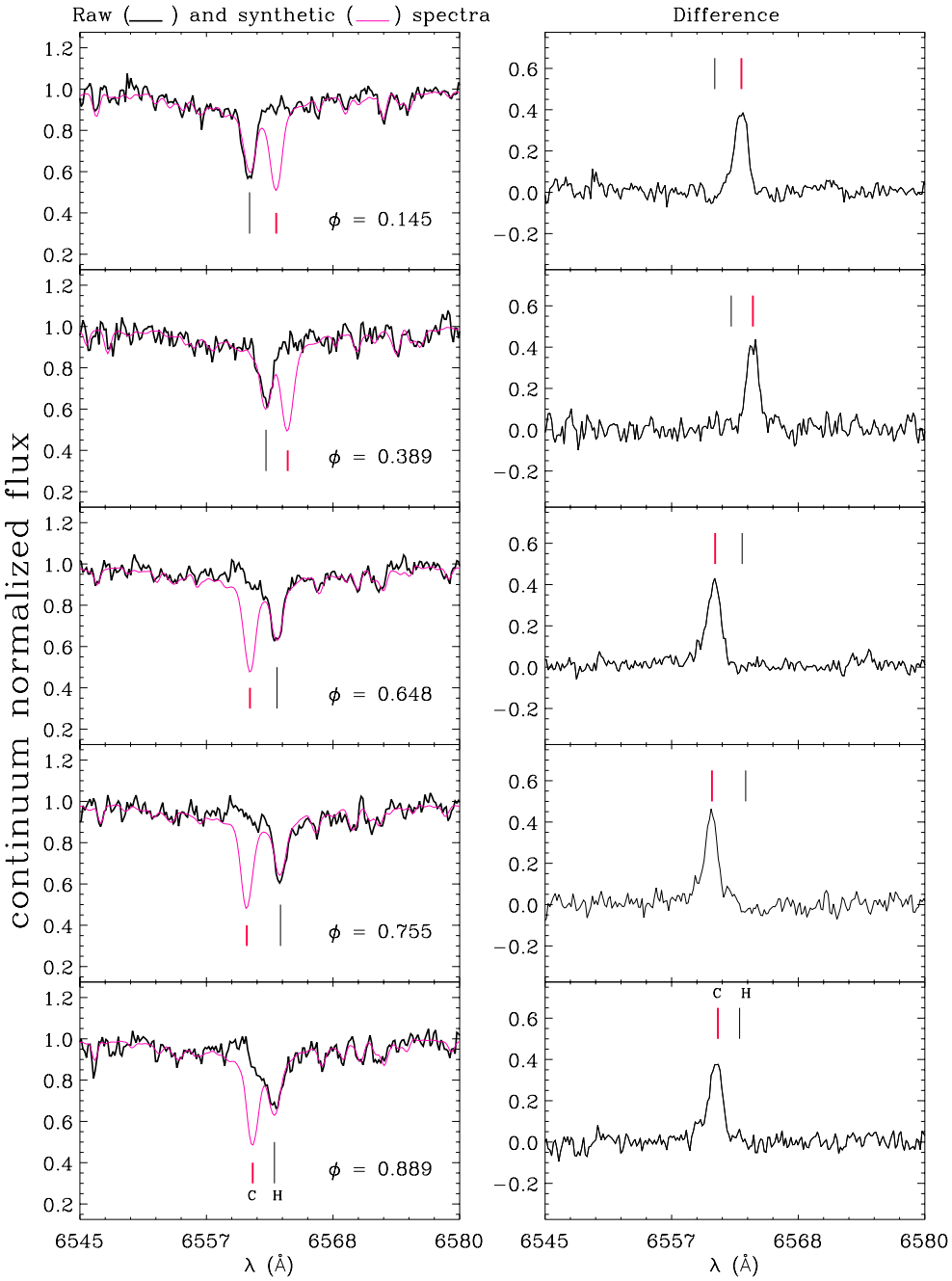

Fig. 8. Sample of Hα spectra of MM Her acquired around the two quadratures. In the left–hand panels the observed spectra are displayed by a thick line, while the synthetic ones are reproduced by thin lines. In the right–hand panels the differences are shown. The phases of observations and the wavelength of the Hα centers of the hot and cool component are also marked.

Another interesting similarity/difference between MM Her and AR Lac is given by the behaviour of the Hα emission. Both systems have components of similar spectral types (G2 V-IV/K0 IV) but different orbital period. In AR Lac both components display chromospheric activity in Ca II, Mg II and Hα (see e.g. Frasca et al. 2000a). This fact could be explained by the stronger dynamo action on the hotter component of AR Lac, because the orbital and rotational period, the system being synchronous, is shorter than that of MM Her (2 days for AR Lac versus 8 days for MM Her). But according to this picture, we should expect a stronger Hα emission also from the K component of AR Lac, while the reverse is true. The excess emission EW from the K0 IV of AR Lac after renormalization to the star continuum is about 0.3 Å (the value reported in Frasca et al. 2000a is referred to the system combined continuum), while the emission of the cool component of MM Her is about 1.1 Å. The two stars are very similar, the mass and radius of the K0 star being $M = 1.27\ M_{\odot}$ and $R = 2.89\ R_{\odot}$ for MM Her (Evren 1987b), and $M = 1.33\ M_{\odot}$ and $R = 2.72\ R_{\odot}$ for AR Lac (Frasca et al. 2000a). So, the only significant

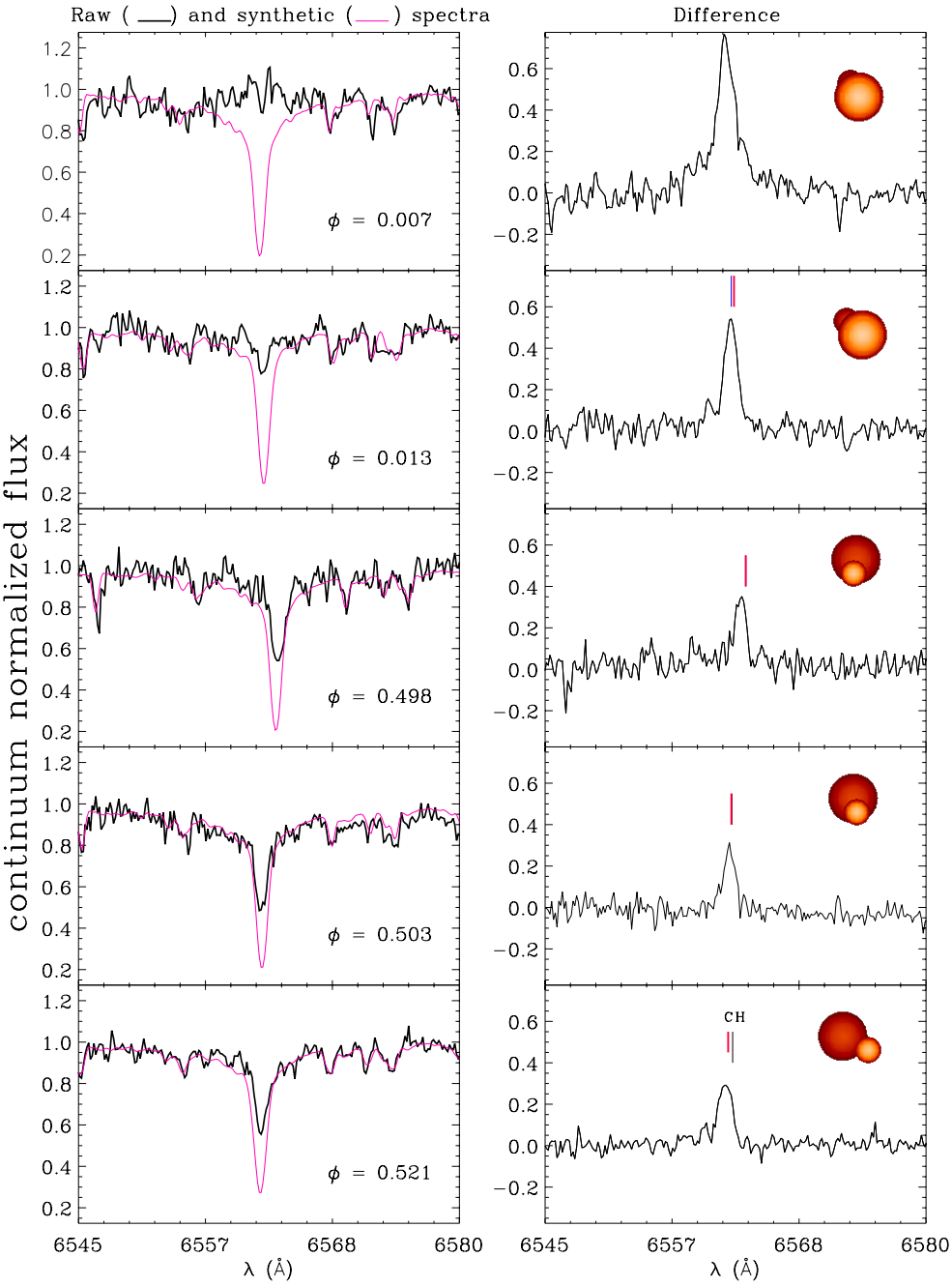

Fig. 9. Sample of Hα spectra of MM Her acquired near the two eclipses. The system configuration, as viewed from the Earth, is sketched on the right-hand side.

difference is the orbital period, i.e. the system separation. For some reason the tidal effect tends to suppress the chromospheric Hα emission, the rotation period working in the opposite sense to what we expect from dynamo theory.

5. Conclusions

From the new light and colour curves obtained in 1998 and 1999, data sets given in Paper I and Hα spectroscopy made in 1999, the following conclusions for MM Her have been obtained:

(1) MM Her has at least two separate spots or spot groups in 1998 and 1999. The effect of the first spot that causes more light loss outside eclipses is seen at phase 0.10, while the effect of the other spot appears at phase 0.62 in 1998. Similar effects on the 1999 light curve are seen at phases 0.05 and 0.43, respectively. The amplitudes of the light variations outside eclipse are about $0\overset{m}{.}04$ and $0\overset{m}{.}05$ in 1998 and 1999, respectively, and are the smallest we have obtained so far.

(2) The displacements of the phases of the second spot obtained in 1998 and 1999 have improved the migration period of Spot 2, leading to a migration period of 5.9 years, very close to that of Spot 1. Both spot groups migrate

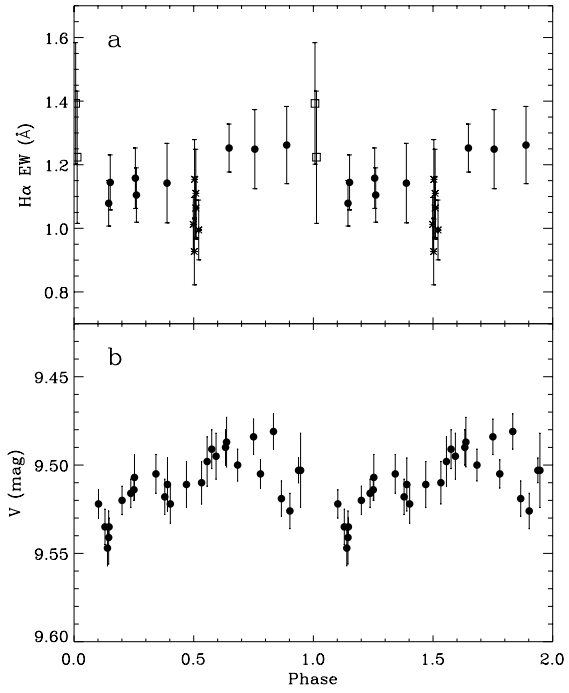

Fig. 10. Hα *EW* **a)** and *V* light **b)** variation of MM Her in 1999. In the upper panel, data acquired near the primary and secondary eclipse are plotted with open squares and asterisk, respectively.

toward smaller orbital phases, i.e. rotate faster than the co-rotation period. In the solar analogy, with rotational angular velocity increasing toward the equator, we suggest that the co-rotation occurs at intermediate latitudes and that spot groups are closer to the equator than the co-rotation latitudes. This is the case, for example, for RS CVn, as shown by the detailed mapping analysis which gives average spot latitudes moving from 25° in the period 1963-1984 to 10° in the period 1988-1993, with the spots always rotating faster than the orbital period (Rodonò et al. 1995).

(3) When the spots located on the cooler component are seen at phase ≈0.50, the amplitude of the light variation is larger than in other phases. This effect is attributed to a greater concentration of spots when the active longitude is on the hemisphere facing the companion. Similar results have been found for AR Lac (Lanza et al. 1998) and II Peg (Berdyugina et al. 1999). One can conclude that the tidal effect seems to enhance the magnetic flux tube emergence and therefore the spot formation.

(4) MM Her certainly shows Hα emission associated only with the K0 IV component. No clear rotational modulation is seen, but the average *EW* emission values at the first quadrature are slightly smaller than those at the second quadrature. This small asymmetry is in the same sense as the light variation.

We have analyzed various causes which may be responsible for such an asymmetry, like faculae on the bright hemisphere or absorbing matter on the trailing hemisphere of the K0 IV component, but the effect is so marginal and close to the size of the observational errors that we are inclined to think that present MM Her data do not show a definite rotational modulation in the Hα chromospheric emission.

Since MM Her is rather an active star, the absence of Hα modulation may be a temporary situation, as observed in other RS CVn systems, for example UX Ari (Catalano et al. 2000).

(5) New radial velocity measurements and orbital parameters have been obtained. A new solution for the system elements leads to a mass difference between the two components that is a little larger than that found by previous authors, but in better agreement with the spectral types of the two stars and their evolutionary stage. The barycentric velocity γ of the system seems to remain constant in time, within the errors.

Acknowledgements. G. Taş would like to thank the Director Prof. M. Rodonò and the staff of Catania Astrophysical Observatory (Mount Etna) for allocation of telescope time and kind hospitality. This work was supported by Ege University Research Fund (Project No. 99/FEN/014). G. Taş is also grateful to the Scientific and Technical Resource Council of Turkey; without their financial support she could not gather the spectroscopic data. This work has been also supported by the Italian *Ministero dell' Università e della Ricerca Scientifica e Tecnologica* and by the *Regione Sicilia* who are gratefully acknowledged. The authors are indepted to the anonymous referee, who made valuable comments on the paper.

References

Amado, P. J., & Byrne, P. B. 1997, A&A, 319, 967
Berdyugina, S. V., & Tuominen, I. 1998, A&A, 336, L25
Berdyugina, S. V., Ilyin, L. Berdyugin, A. V., & Tuominen, I. 1999, A&A, 350, 626
Bopp, B. W., & Talcott, J. C. 1978, AJ, 83, 1517
Budding, E., & Zeilik, M. 1987, ApJ, 319, 827
Byrne, P. B., Abdul Aziz, H., Amado, P. J., et al. 1998, A&AS, 127, 505
Carlos, R. C., & Popper, D. M. 1971, PASP, 83, 504
Catalano, S., Rodonò, M., Frasca, A., & Cutispoto, G. 1996, in Stellar Surface Structure, ed. K. G. Strassmeier, & J. Linsky, IAU Symp., 176, 403
Catalano, S., Rodonò, M., Cutispoto, G., et al. 2000, in Variable Stars as Essential Astrophysical Tools, ed. C. İbanoğlu (Kluwer Academic Publishers), 687
Dorren, J. D., & Guinan, E. F. 1990, ApJ, 348, 703
Doyle, J. G., Byrne, P. B., & Van den Oord, G. H. J. 1989, A&A, 224, 153
Evans, D. S. 1979, IAU Symp., 30, 57
Evren, S. 1985, Ap&SS, 108, 113
Evren, S. 1986, Ph.D. Thesis, Ege University, Bornova, Izmir
Evren, S. 1987a, Ap&SS, 137, 151
Evren, S. 1987b, Ap&SS, 137, 357
Evren, S., & Taş, G. 1999, IBVS, 4687
Foukal, P., & Lean, J. 1986, ApJ, 302, 826
Foukal, P. 1987, Ap&SS, 229, 185
Foukal, P., & Lean, J. 1988, ApJ, 328, 347
Frasca, A., Marino, G., Catalano, S., & Marilli, E. 2000a, A&A, 358, 1007

Frasca, A., Freire Ferrero, R., Marilli, E., & Catalano, S. 2000b, A&A, 364, 179
Hall, D. S. 1992, in Robotic Telescopes in the 1990s, ASP Conf. Ser. 34, ed. A. V. Filippenko, 27
Hall, D. S., Henry, G. W., Burke, E. W., & Mullis, J. L. 1977, IBVS, 1311
Hall, J. C., & Ramsey, L. W. 1992, AJ, 104, 1942
Heckert, P. A., & Ordway, J. I. 1995, AJ, 109, 2169
Henry, G. W., Eaton, J. A., Hamer, J., & Hall, D. S. 1995, Ap&SS, 229, 185
Imbert, M. 1971, A&A, 12, 155
Lanza, A. F., Catalano, S., Cutispoto, G., Pagano, I., & Rodonò, M. 1998, A&A, 332, 541
Lean, J., & Foukal, P. 1988, Science, 240, 906
Mohin, S., & Raveendran, A. V. 1989, J. Astrophys. Astron., 10, 35
Montes, D., Fernandez-Figueroa, M. J., de Castro, E., & Sanz-Forcada, J. 1997, A&AS, 125, 263
Olah, K., Hall, D. S., & Henry, G. W. 1991, A&A, 251, 531
Oliver, J. P. 1974, Ph.D. Thesis, University of California, Los Angeles
Popper, D. 1980, ARA&A, 18, 115
Popper, D. 1988, AJ, 96, 1040
Ramsey, L. W., & Nation, H. L. 1984, AJ, 89, 115
Raveendran, A. V., & Mohin, S. 1995, A&A, 301, 788
Rodonò, M., Byrne, P. B., Neff, J. E., et al. 1987, A&A, 176, 267
Rodonò, M., & Cutispoto, G. 1992, A&AS, 95, 55
Rodonò, M., Lanza, A. F., & Catalano, S. 1995, A&A, 301, 75
Sowell, J. R., Hall, D. S., Henry, G. W., Burke, E. W., & Jr. Milone, E. F. 1983, Ap&SS, 90, 421
Stauffer, J. R. 1980, AJ, 85, 1341
Strassmeier, K. G., Hall, D. S., Fekel, F. C., & Scheck, M. 1993a, A&AS, 100, 173
Strassmeier, K. G., Rice, J. B., Wehlau, W. H., Hill, G. M., & Matthews, J. M. 1993b, A&A, 268, 671
Strassmeier, K. G. 1994, A&A, 281, 395
Taş, G. 2000a, IBVS, No. 4883
Taş, G. 2000b, IBVS, No. 4901
Taş, G., Evren, S., & İbanoğlu, C. 1999, A&A, 349, 546, Paper I
Tonry, J., & Davis, M. 1979, AJ, 84, 1511
Topping, J. 1972, Errors of Observation and Their Treatment (Chapman and Hall Ltd.), 89
Tsesevich, V. P. 1954, Odessa Izv. 4, Part 2, 116
Turner, D. G. 1979, PASP, 91, 642
Weiler, E. J. 1978, MNRAS, 182, 77